Scanning tunneling microscopy of the blue bronzes $(Rb,K)_{0.3}MoO_3$

U. Walter*
Department of Physics, University of California, Berkeley, California 94720

R. E. Thomson
Department of Physics, University of California, Berkeley, California 94720
and Materials Science Division, Lawrence Berkeley Laboratory, Berkeley, California 94720

B. Burk, M. F. Crommie, and A. Zettl
Department of Physics, University of California, Berkeley, California 94720

John Clarke
Department of Physics, University of California, Berkeley, California 94720
and Materials Science Division, Lawrence Berkeley Laboratory, Berkeley, California 94720
(Received 15 July 1991)

We have performed scanning tunneling microscopy of the blue bronzes $K_{0.30}MoO_3$ and $Rb_{0.30}MoO_3$ both above and below the charge-density-wave (CDW) transition temperature, $T_P = 180$ K. We were able to image the Mo-O octahedra on the crystal surface at 295, 143, and 77 K. Below T_P, we were not able to image any additional superstructure due to the CDW, suggesting a relatively small CDW amplitude at the sample surface. Furthermore, the lattice images that we obtained below T_P are unaffected by the sliding of the CDW.

I. INTRODUCTION

The scanning tunneling microscope (STM) is a sensitive tool for investigating electronic as well as topographic structures of surfaces. Since the tunneling current of an STM depends on the electronic density of states at the Fermi level, it can image charge-density waves (CDW's) at the surface of a conducting or semiconducting Peierls-distorted crystal.[1-3] In principle, it is possible to use an STM not only to study the static CDW, but also to investigate the CDW dynamics. For example, a Fröhlich-mode sliding CDW induced by a bias electric field should be accessible to a STM, provided that the surface CDW is not pinned excessively strongly.

There are only a few systems known to show Fröhlich conductivity at reasonably low electric fields. These include $(TaSe_4)_2I$, $(NbSe_4)_{10/3}I$, $NbSe_3$, TaS_3, and the two blue bronzes $K_{0.30}MoO_3$ and $Rb_{0.30}MoO_3$. The transition-metal trichalcogenides $NbSe_3$ and TaS_3 grow in needlelike crystals typically less than 100 μm in diameter, making them difficult to use as STM specimens. The halogenated transition-metal tetrachalcogenides $(TaSe_4)_2I$ and $(NbSe_4)_{10/3}I$ have quasi-two-dimensional crystal structure and are therefore candidates for STM studies, but their rapid oxidation complicates the surface studies. The blue bronzes, on the other hand, form large cleavable crystals that are relatively inert, making them practical specimens for STM experiments. Recently, two groups[4,5] have published STM images of blue bronze at room temperature which is above the CDW transition temperature, $T_P = 180$ K.

We have attempted to image the CDW in blue bronze at temperatures below T_P. Although we obtained images displaying the lattice structure at 295, 143, and 77 K, we were unable to find evidence for the CDW. In this paper we relate the surface lattice structure to the bulk, describe the surface CDW structure that we expect from x-ray-diffraction and neutron-scattering results, and discuss possible reasons why we did not observe the CDW in our STM images. We have published a preliminary report of this work elsewhere.[6]

II. THE BLUE BRONZES

The blue bronzes, M_xMoO_3 ($0.24 < x < 0.30$, M = Na, K, and Rb), crystallize into the monoclinic $C2/m$ structure with $a_0 = 18.25$ Å (18.94 Å), $b_0 = 7.560$ Å (7.560 Å), $c_0 = 9.855$ Å (10.040 Å), and $\gamma = 117.53°$ (118.83°) with 20 formula units per unit cell for $K_{0.30}MoO_3$ ($Rb_{0.30}MoO_3$).[7,8] These compounds form a layered structure with sheets of distorted MoO_6 octahedra (corner shared) separated by, but also held together by, the alkali-metal atoms. These sheets are composed of units of ten octahedra, eight of which share edges to form a zig-zag chain in the [102] direction. The extra two octahedra, referred to as the "hump" octahedra in Ref. 9, share an adjoining edge with two of the chain octahedra, making them slightly displaced from the chain octahedra. These units of ten octahedra in turn share corners of the chain octahedra of adjoining unit cells to form infinite Mo-O sheets parallel to the b and [102] plane.

Because the bonds between the sheets are weak, the crystals are easily cleaved parallel to the b and [102] plane. For concentrations of $x < 0.30$ the blue bronzes are nonstochiometric because not all of the interstitial (interlayer) positions are occupied by the M atoms. For

$x = \frac{1}{3}$ the neighboring phase of semiconducting red bronze is formed.

Below $T_P = 180$ K an incommensurate CDW is formed in the blue bronzes. This creates a gap in the conduction band and therefore gives rise to semiconducting behavior below T_P.[10] The phase transition affects nearly all microscopic and macroscopic quantities measured below T_P. A CDW in blue bronze was postulated by Travaglini *et al.*[11] in 1981 and was subsequently confirmed by nonlinear electronic transport measurements[12] and by measurement of a Kohn anomaly in the molybdenum-oxygen octahedra along the b^* direction.[13,14] Recently, it was suggested that below $T = 100$ K the CDW undergoes an incommensurate-commensurate phase transition,[15] although the occurrence of such a "lock-in" transition is still controversial. The threshold field for depinning the CDW, E_T, varies from 50 to over 250 mV/cm for $T > 25$ K.[16]

The structural and transport properties of $K_{0.30}MoO_3$ and $Rb_{0.30}MoO_3$ are very similar above and below T_P, which is identical in the two materials. The STM images of the two types of blue bronze are also nearly identical. Thus all results described for $K_{0.30}MoO_3$ in the following discussion also apply to $Rb_{0.30}MoO_3$.

III. EXPERIMENTAL PROCEDURE AND RESULTS

We performed our experiments with an STM, developed for low-temperature measurements, which we have described elsewhere.[2] Most of our images were recorded in the constant-height mode, each image being acquired in about 1.5 s. We obtained images above the transition at 295 K, in the incommensurate phase at 143 K (using a pentane ice bath), and in the proposed commensurate phase at 77 K.

We prepared single crystals of both K and Rb blue bronze for the microscope by evaporating three indium contacts onto the crystals before mounting them on copper sample holders with stycast epoxy (Fig. 1). One contact on the center of the rear side of the crystal was used for the tunneling bias voltage. The other two contacts on each end of the top side of the crystal enabled us to apply the electric field necessary to induce Fröhlich conductivity at low temperatures. We scored the crystal with a razor blade before cleaving it with tape; the epoxy protected the contacts during the cleaving process.

Initial test runs with samples cleaved in air did not produce images with atomic resolution. Instead, we obtained pictures showing large structures that were stable but not periodic (Fig. 2). We attributed these structures to surface contamination and subsequently worked with samples either cleaved and handled in clean N_2 gas or cleaved under hexadecane. In the latter case, images at room temperature were obtained with the hexadecane remaining on the surface. We obtained low-temperature images by dissolving the hexadecane in pentane and working in a bath of pentane at its melting point (143 K). These cleaner samples yielded images with lattice resolution at all three temperatures (see Figs. 3–5).

Figure 3 is an example of the images we obtained at room temperature. The clear periodic structure in this image reflects the periodicity of the rhomboid unit cell of blue bronze. An analysis of 14 images taken at 295 K (from nine samples) yields values of nearest-neighbor distances of 7.4 ± 0.3 and 10.4 ± 0.4 Å and an angle between the two nearest-neighbor directions of $68° \pm 3°$. Our calculations from x-ray-diffraction data on $K_{0.30}MoO_3$ yield a surface unit cell with crystal lattice translation vectors of 7.56 Å in the b direction and 10.56 Å in the [112] direction. The angle between these two lattice vectors is 69°. Thus, within our experimental error, the structure observed in the STM images agrees with the calculated crystal surface lattice translation vectors with regard to both the lattice constants and the angle.

Figures 4 and 5 are images of the sample in the proposed commensurate phase (77 K) and in the incommensurate phase (143 K), respectively. (Figure 5 is the only image shown in this paper that was taken in the constant-current mode and took about 30 s to acquire.) Comparing either figure with Fig. 3, we conclude that we are again imaging merely the surface lattice unit cell with no evidence of the CDW. An analysis of seven images (from five samples) taken at 77 and 143 K yielded lattice constants of 7.3 ± 0.6 and 10.7 ± 0.4 Å and an angle of

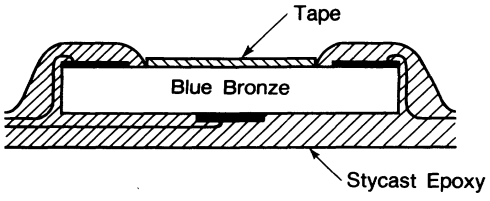

FIG. 1. Schematic of the sample mounted for the STM. The stycast epoxy protects the evaporated indium contacts while the sample is cleaved with tape.

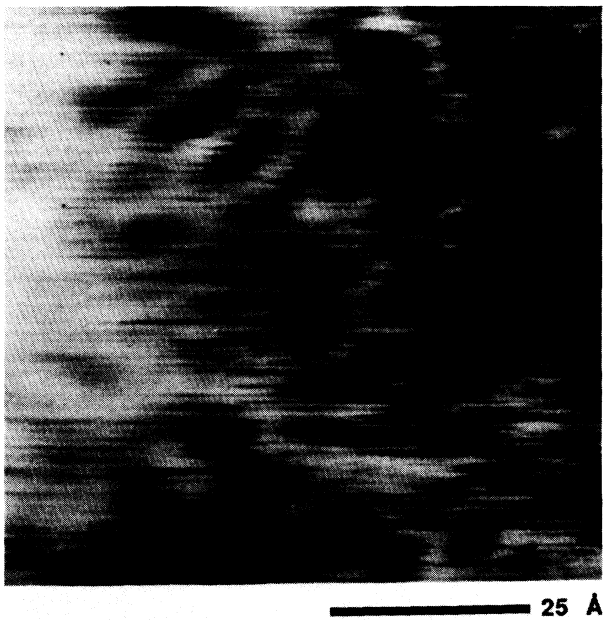

FIG. 2. STM image of the contaminated $K_{0.30}MoO_3$ surface at 143 K.

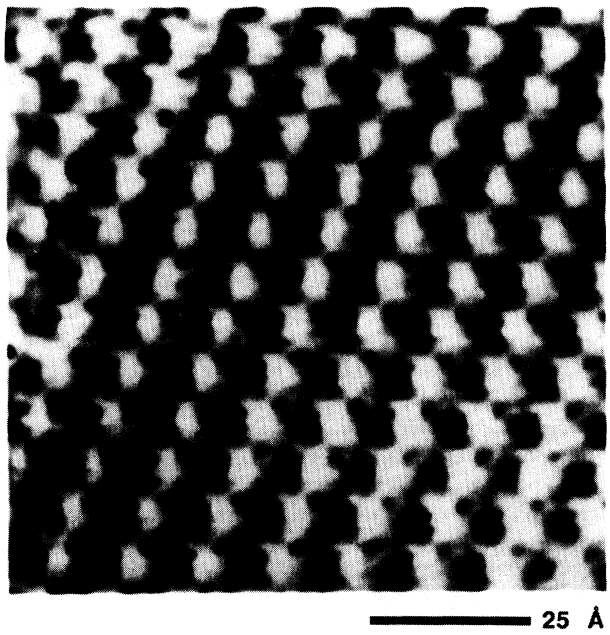

FIG. 3. STM image of $K_{0.30}MoO_3$ at 295 K. A single maximum per surface unit cell is resolved.

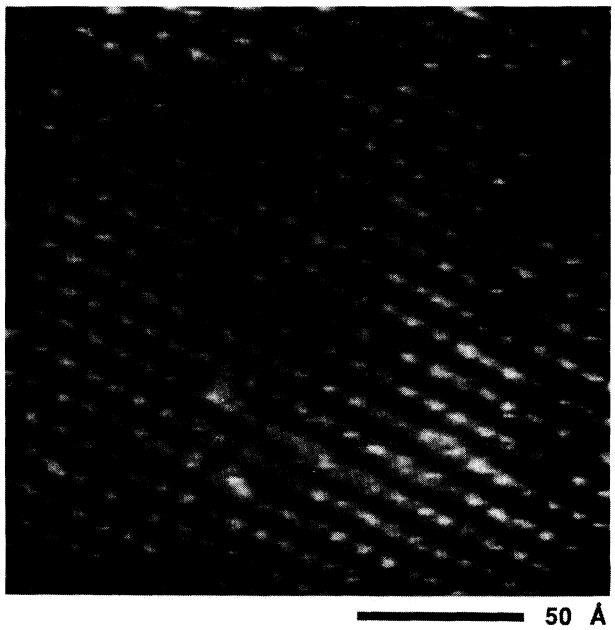

FIG. 5. STM image of $K_{0.30}MoO_3$ in the incommensurate phase at 143 K.

68°±4°. These lengths agree with the distances and angle given for the atomic lattice but do not agree with those calculated from x-ray-diffraction and neutron-scattering data[13,15,17] for the CDW in the cleavage plane, 10.2 and 11.1 Å and an angle of 62.6° (see the Appendix). There is no indication of any superstructure we could attribute to the CDW.

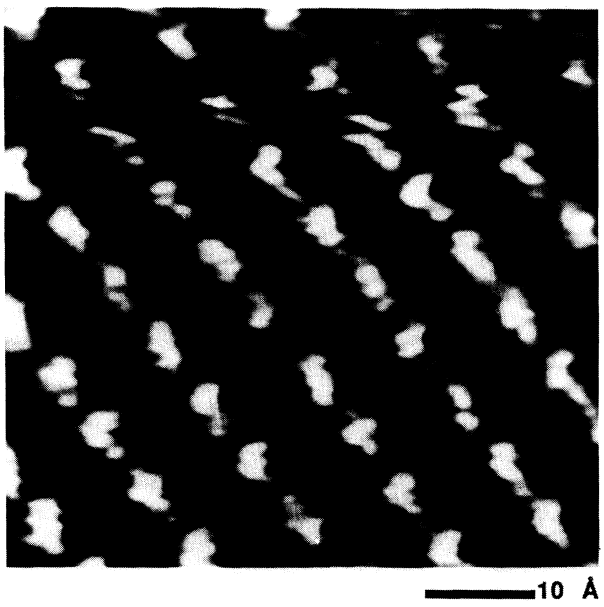

FIG. 4. STM image of $K_{0.30}MoO_3$ in the proposed commensurate phase at 77 K. The image shows only the periodicity of the surface lattice unit cell and does not display any structure due to the CDW.

In another attempt to find evidence of the CDW we Fourier transformed our images as shown, for example, in Fig. 6(a), which is a Fourier transform of Fig. 5. For comparison, in Fig. 6(b) we display the Fourier transform showing the position of the peaks for the atomic lattice and the CDW calculated from x-ray-diffraction and neutron-scattering data.[13,15,17] A careful examination of Figs. 6(a) and 6(b) shows that the peaks from our STM image agree well with those calculated for the atomic lattice, but that there are no discernible peaks corresponding to the CDW structure.

In a further attempt to see some signature of the CDW, we applied an independently grounded voltage of 200 mV to the two side contacts on the top surface of the crystal to produce an electric field three times the threshold field E_T (determined by a measurement of dV/dI on the same sample). This procedure did not extinguish or modify the structures observed by the STM at either of the lower temperatures. Therefore, we conclude that none of our STM images shows any evidence of the CDW superstructure.

IV. DISCUSSION

The inability of our STM to detect a CDW in blue bronze implies that the charge modulation at the surface is nonexistent or at least too weak to be detected. There appear to be at least two possible explanations for this observation. The first of these is that the CDW is attenuated near the surface. It is well known that the characteristics and behavior of the CDW at the surface can be significantly different from those in the bulk material.[18–21] In fact, it would be surprising for the CDW to extend unchanged to the surface, since one expects prop-

erties that are known to affect the CDW to be quite different on the surface from their values in the bulk. These properties include the impurity concentration and nonstoichiometry of the crystal, as well as the modified electronic structure at the surface. This last effect is especially important in blue bronze, where we expect that some of the alkali-metal atoms do not remain at the surface after cleaving.[22] Also, several studies have indicated that the pinning mechanisms of CDW motion may be influenced by surface effects,[18–20] such as increased scattering of carriers by the surface or pinning by defects or different CDW wave vectors at the surface.

Alternatively, the CDW, as measured by STM, may be weak or absent on the surface because it is concentrated on those Mo-O octahedra that are significantly below the surface. Figure 7 is a schematic of the structure of blue bronze showing the relative displacements (due to the Kohn anomaly) of the atoms in the (010) plane from their room-temperature positions (after Sato *et al.*[13]). The top edge of the drawing, which we refer to as the "surface," is defined by the positions of the alkali-metal ions (closed circles) before the cleaving process. (The fact that these ions may have been removed during cleaving is not relevant to the argument, which concerns the relative distances of the various atoms from the surface.) The Mo atoms closest to the "surface" are 1.8 Å below the "surface" and those that undergo the largest displacements are 3.5 Å below the "surface." If the CDW is concentrated on the same atoms that are displaced due to the Kohn anomaly, as one would expect, it may be that the greater part of the CDW modulation is too far below the surface to be detected with our STM.

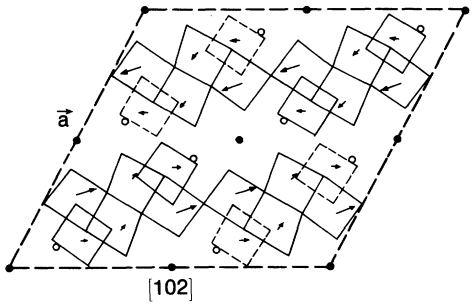

FIG. 7. Side view of a single unit cell of blue bronze projected onto the plane perpendicular to the *b* axis. The "surface" of the crystal (defined by the *b* and [102] plane) is along the top of the figure. Closed circles are the K atoms in the uppermost positions. Open circles are the K atoms 1.2 Å below the "surface." The Mo atoms are at the center of the oxygen octahedra and the three highest sets lie at levels 1.8, 2.4, and 3.5 Å below the "surface." The arrows indicate the relative amplitudes and directions of the displacement of the Mo atoms due to the CDW [after Sato *et al.* (Ref. 13)].

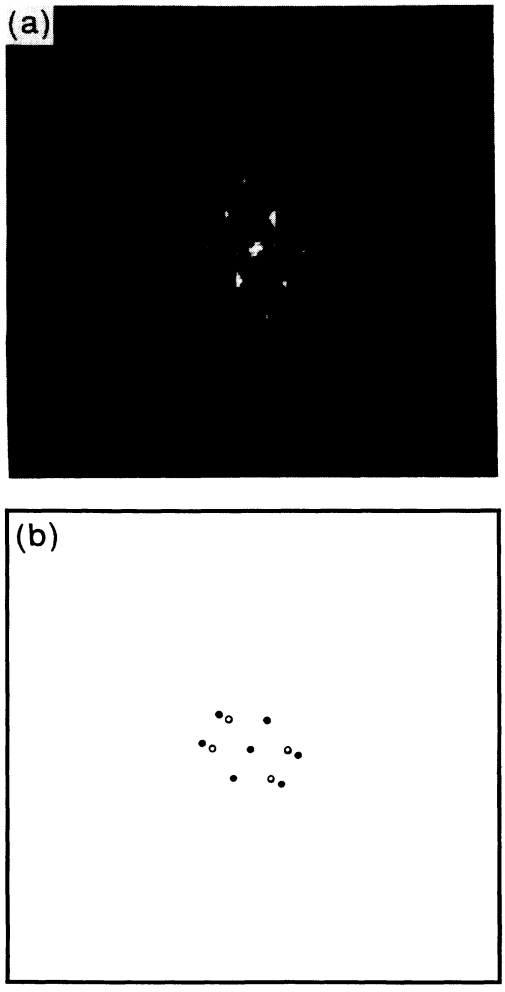

FIG. 6. (a) Fourier transform of Fig. 5 showing the atomic lattice peaks. The two weak peaks nearest the center of the transform are due to 60-Hz noise on the feedback signal. (b) Schematic showing the calculated positions of the atomic lattice peaks (closed circles) and the CDW peaks (open circles).

Given our result that the CDW on the surface of blue bronze is either weak or nonexistent, it is of interest to consider previous work relevant to this problem. In 1990, Zhu *et al.*[21] reported that the CDW in blue bronze was easily detected by grazing-incidence x-ray diffraction. In this study, the CDW satellite peak was unchanged at the shallowest incident angle used, which was calculated to have an x-ray penetration depth of 20 Å, corresponding to about 2.5 Mo-O sheets. If our STM fails to image the CDW because it does not propagate to the surface, then to be consistent with the study of grazing-incidence x-ray diffraction we have to conclude that the CDW disappears within the last Mo-O sheet. However, our second proposed explanation for our results, that the CDW is concentrated on the Mo atoms which are too far below the surface for our STM to image the CDW, is also consistent with the x-ray results.

Our failure to detect the CDW appears to contradict the results of Nomura and Ichimura,[23] who detected a peak in the frequency spectrum of the STM tunneling current which they attributed to the presence of a sliding CDW on the surface of a sample biased above its CDW conduction threshold field. However, these authors were unable to obtain STM images of either the CDW or the atomic lattice. It is possible that the peak that they ob-

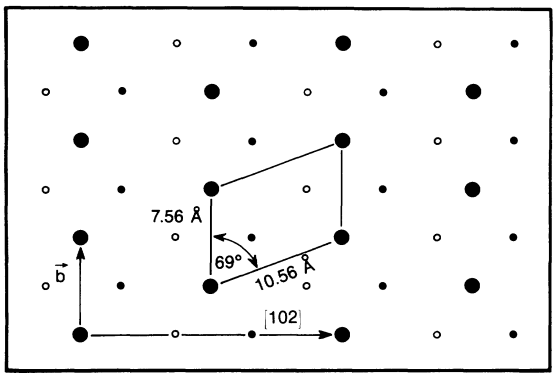

FIG. 8. Positions of K atoms projected onto the b and [102] plane (the cleavage plane) calculated from x-ray-diffraction data. Large closed circles indicate atoms in this plane. Small open circles indicate atoms 1.2 Å below the plane, and small closed circles indicate atoms 1.2 Å above the plane.

served in the frequency spectrum was due to a time-varying voltage (i.e., narrow band noise) induced across the sample by the sliding CDW. This oscillating voltage could have modulated the tip-sample bias voltage of the STM, and hence the tunneling current.

Finally, one might ask what aspect of the atomic lattice the STM images in blue bronze. The periodicity of the STM images reflects the periodicity of the unit cell of the material, but one would like to know which part of the unit cell, the K atoms or the Mo-O octahedra, is being imaged. An inspection of Figs. 8 and 9 reveals that the uppermost potassium atoms and the uppermost Mo-O octahedra (the "hump" octahedra of Ref. 9) both produce lattices with identical unit-cell vectors (the known surface lattice translation vectors), making it impossible to differentiate between them from their measured periodicities. However, from an analysis of the calculated electronic density of states,[9] it seems unlikely that the alkali-metal ions would affect the tunneling current, since they have no electronic states available near the Fermi level. Also, since the blue bronzes are generally nonstochiometric, not all of the interstitial (interlayer)

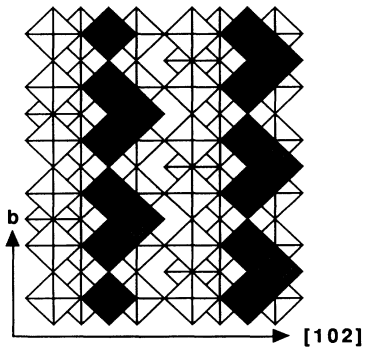

FIG. 9. Structure of the idealized Mo-O octahedra in the topmost unit cell of the cleavage plane. The centers of the "hump" octahedra (the rightmost octahedron in a shaded group of three) are 1.8 Å below the "surface" defined by the b and [102] plane. The gray octahedra have centers 2.4 Å below the "surface."

positions are expected to be occupied by alkali-metal atoms. Thus, if we were imaging the K ions, we would expect a very large number of defects, contrary to our observations. Therefore, we conclude that the periodic structure in our STM images is due to the Mo-O octahedra. In this case, we may be imaging just the uppermost "hump" octahedra (the dark gray octahedra in Fig. 9), or, alternatively, each maximum in the STM image may correspond to a blurred image of a group of three Mo-O octahedra (both the dark and light-gray octahedra in Fig. 9). The latter option was the hypothesis of Heil *et al.*[4] for their room-temperature STM data, and Anselmetti *et al.*[5] concluded that it was at least consistent with their data.

In conclusion, we have used our STM to image the atomic lattice in the blue bronzes above the CDW transition temperature (295 K), in the incommensurate phase (143 K) and in the proposed commensurate phase (77 K). At all three temperatures the structure imaged by the STM is consistent with the surface crystal structure of the uppermost "hump" octahedra. However, we have not seen any evidence for the CDW's known to exist in these materials at the lower temperatures. The two most likely reasons for this fact are that either the CDW is attenuated at the surface of the crystal, or that the CDW is concentrated on the Mo-O octahedra and is therefore too far below the surface to be imaged with our STM.

ACKNOWLEDGMENTS

We thank R. V. Coleman for useful discussions, and J. Heil for sending us results of their work (Ref. 4) prior to publication. This work was supported by the Director, Office of Energy Research, Office of Basic Energy Science, Materials Science Division of the U. S. Department of Energy, under Contract No. DE-AC03-76F00098 and by NSF Grant No. DMR-90-17254. One of us (U.W.) acknowledges the financial support of the Deutsche Forschungsgemeinschaft (DFG).

APPENDIX: CALCULATION OF THE SURFACE CDW STRUCTURE

We have calculated the projection of the CDW on to the cleavage plane in order to compare the CDW periodicity to the observed periodicity of our STM images. The cleavage plane in blue bronze is defined by the b and [102] crystal axes, and the CDW wave vector is known from x-ray-diffraction and neutron-scattering data to be[13,15,17]

$$\mathbf{q}_{\mathrm{CDW}}^{\pm}=\pm\delta\mathbf{b}^{*}+0.5\mathbf{c}^{*} ,$$

where $\delta=0.737$ (0.74) for $K_{0.3}MoO_3$ ($Rb_{0.3}MoO_3$). Projection of the CDW wave vector onto $\mathbf{b}$ gives

$$\mathbf{q}_{\mathrm{CDW}}^{\pm}\cdot\frac{\mathbf{b}}{|b|}=(\pm\delta\mathbf{b}^{*}+0.5\mathbf{c}^{*})\cdot\frac{\mathbf{b}}{|b|}$$

$$=\pm\delta\mathbf{b}^{*}\cdot\frac{\mathbf{b}}{|b|}=\pm\frac{2\pi\delta}{|b|} ,$$

while projection of the CDW wave vector on to [102] gives

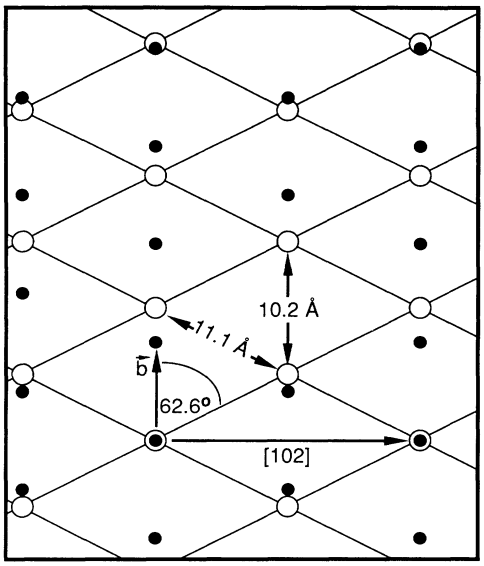

FIG. 10. The incommensurate charge-density wave of $K_{0.30}MoO_3$ in the b and [102] plane calculated from x-ray-diffraction and neutron-scattering data. The solid lines indicate the CDW wave front with a wavelength of 9.07 Å, and the open circles indicate the CDW maxima. Closed circles indicate the positions of the "hump" Mo-O octahedra.

$$\mathbf{q}^{\pm}_{\mathrm{CDW}}\cdot\frac{\mathbf{a}+2\mathbf{c}}{|\mathbf{a}+2\mathbf{c}|}=(\pm\delta\mathbf{b}^*+0.5\mathbf{c}^*)\cdot\frac{\mathbf{a}+2\mathbf{c}}{|\mathbf{a}+2\mathbf{c}|}$$
$$=\mathbf{c}^*\cdot\frac{\mathbf{c}}{|\mathbf{a}+2\mathbf{c}|}=\frac{2\pi}{|\mathbf{a}+2\mathbf{c}|}\ .$$

Thus, in the cleavage plane we find

$$\mathbf{q}^{\pm}_{\mathrm{project}}=2\pi\left[\frac{\pm\delta}{|b|}\frac{\mathbf{b}}{|b|}+\frac{1}{|\mathbf{a}+2\mathbf{c}|}\frac{\mathbf{a}+2\mathbf{c}}{|\mathbf{a}+2\mathbf{c}|}\right]\ .$$

The translation vectors reciprocal to the projected wave vectors are

$$\mathbf{T}^{\pm}_{\mathrm{project}}=\left[\frac{\pm\mathbf{b}}{2\delta}+\frac{\mathbf{a}+2\mathbf{c}}{2}\right]\ .$$

An equivalent basis for the projected CDW translation vectors is

$$\mathbf{T}^{1}_{\mathrm{project}}=\left[\frac{\mathbf{b}}{\delta}\right];\quad \mathbf{T}^{2}_{\mathrm{project}}=\left[\frac{\mathbf{b}}{2\delta}+\frac{\mathbf{a}+2\mathbf{c}}{2}\right]\ .$$

Finally, the vector magnitudes and angle between the vectors are:

$$|\mathbf{T}^{1}_{\mathrm{project}}|=10.2\ \text{Å}\ ;$$

$$|\mathbf{T}^{2}_{\mathrm{project}}|=11.1\ \text{Å}\ ;\quad \theta=62.6^\circ\ .$$

In Fig. 10 the CDW surface structure is displayed together with the positions of the "hump" octahedra. The CDW forms a superlattice in the cleavage plane that is commensurate in the [102] direction and nearly commensurate in the b direction. In this figure the phase of the CDW with respect to the "hump" octahedra is chosen so that a CDW maximum (open circle) coincides with a "hump" octahedron (closed circle) in the lower-left region of the figure. The choice of the CDW phase is arbitrary in the b direction since the CDW is incommensurate in this direction. In the [102] direction the CDW is commensurate and the phase is chosen so that commensurability is obvious; however, the phase of the CDW may be offset in the [102] direction so that CDW maxima may not coincide with "hump" octahedra.

*Present address: Deutsche Forschungsanstalt für Luft- und Raumfahrt, Linder Höhe, 5000 Köln 90, FRG.

[1]R. V. Coleman, B. Drake, P. K. Hansma, and G. Slough, Phys. Rev. Lett. **55**, 394 (1985).
[2]R. E. Thomson, U. Walter, E. Ganz, J. Clarke, A. Zettl, P. Rauch, and F. J. DiSalvo, Phys. Rev. B **38**, 10 734 (1988).
[3]R. V. Coleman, B. Giambattista, P. K. Hansma, A. Johnson, W. W. McNairy, and C. G. Slough, Adv. Phys. **37**, 559 (1988).
[4]J. Heil, J. Wesner, B. Lommel, W. Assmus, and W. Grill, J. Appl. Phys. **65**, 5220 (1989).
[5]D. Anselmetti, R. Wiesendanger, H.-J. Güntherodt, and G. Grüner, Europhys. Lett. **12**, 241 (1990).
[6]A. Zettl, L. C. Bourne, J. Clarke, M. F. Crommie, M. F. Hundley, R. E. Thomson, and U. Walter, Synth. Met. **29**, F445 (1989).
[7]J. Graham and A. D. Wadsley, Acta Crystallogr. **20**, 93 (1966).
[8]J.-M. Reau, C. Fouassier, and P. Hagenmuller, Bull. Soc. Chim. France **8**, 2883 (1971).
[9]W. H. Whangbo and L. F. Schneemeyer, Inorg. Chem. **25**, 2424 (1986).
[10]W. Fogle and J. H. Perlstein, Phys. Rev. B **6**, 1402 (1972).
[11]G. Travaglini, P. Wachter, J. Marcus, and C. Schlenker, Solid State Commun. **37**, 599 (1981).
[12]J. Dumas, C. Schlenker, J. Marcus, and R. Buder, Phys. Rev. Lett. **50**, 757 (1983).
[13]M. Sato, H. Fujishita, S. Sato, and S. Hoshino, J. Phys. C **18**, 2603 (1985).
[14]C. Escribe-Filippini, J. P Pouget, R. Currat, B. H. Hennion, and J. Marcus, in *Charge Density Waves in Solids,* edited by Gy. Hutiray and J. Solyom Lecture Notes in Physics Vol. 217 (Springer-Verlag, Berlin, 1985), pp. 71–75.
[15]R. M. Fleming, L. F. Schneemeyer, and D. E. Moncton, Phys. Rev. B **31**, 899 (1985).
[16]R. M. Fleming, R. J. Cava, L. F. Schneemeyer, E. A. Reitman, and R. G. Dunn, Phys. Rev. B **33**, 5450 (1986).
[17]J. P. Pouget, C. Noguera, A. H. Moudden, and R. Moret, J. Phys. (Paris) **46**, 1731 (1985).
[18]P. J. Yetman and J. C. Gill, Solid State Commun. **62**, 201 (1987).
[19]J. McCarten, M. Maher, T. L. Adelman, and R. E. Thorne,

Phys. Rev. Lett. **63**, 2841 (1989).
[20]J. C. Gill, Europhys. Lett. **11**, 175 (1990).
[21]X.-M. Zhu, R. Moret, H. Zabel, I. K. Robinson, E. Vlieg, and R. M. Fleming, Phys. Rev. B **42**, 8791 (1990).
[22]We expect that at least the K atoms in the *b* and [102] plane (those in the *d* positions; see Ref. 7) will not remain in their precleavage positions since one-half of the electrostatic forces holding them in place have been removed by cleaving.
[23]K. Nomura and K. Ichimura, Solid State Commun. **71**, 149 (1989).

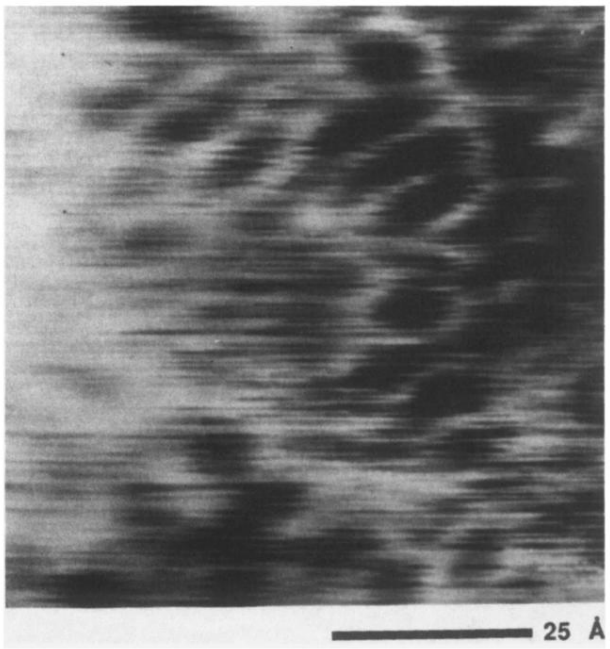

FIG. 2. STM image of the contaminated $K_{0.30}MoO_3$ surface at 143 K.

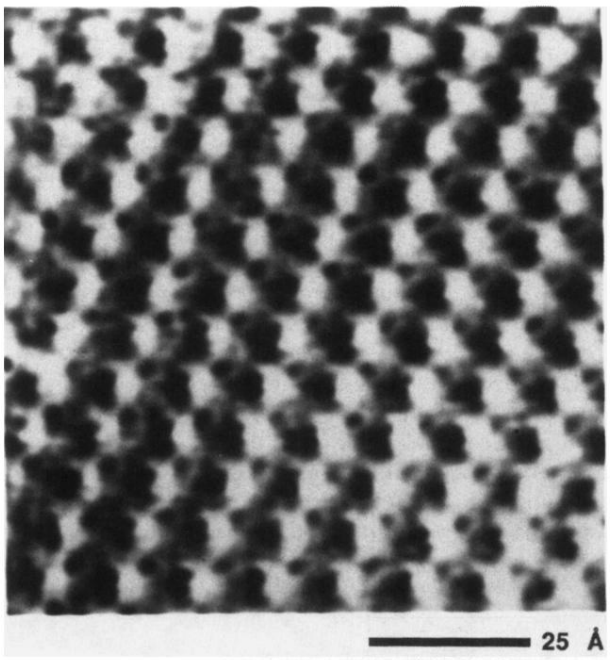

FIG. 3. STM image of $K_{0.30}MoO_3$ at 295 K. A single maximum per surface unit cell is resolved.

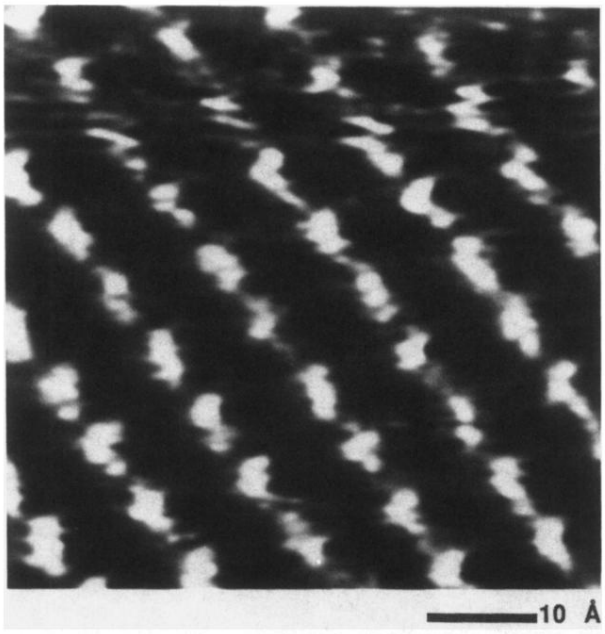

FIG. 4. STM image of $K_{0.30}MoO_3$ in the proposed commen surate phase at 77 K. The image shows only the periodicity of the surface lattice unit cell and does not display any structure due to the CDW.

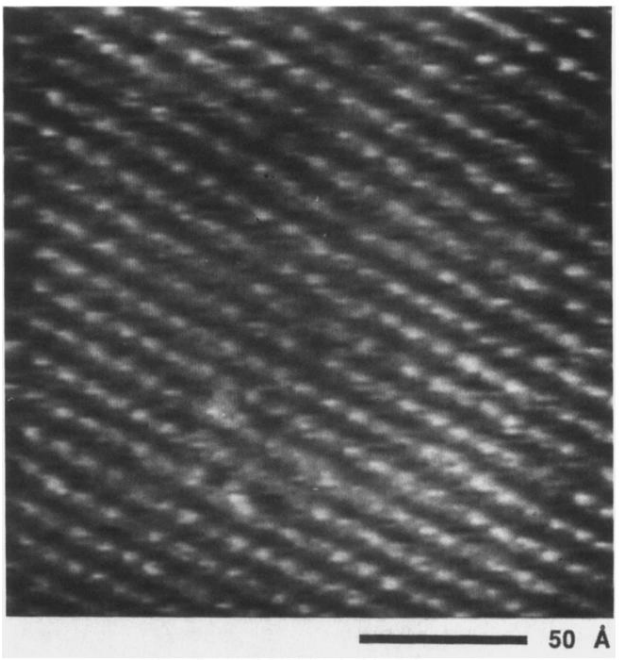

FIG. 5. STM image of $K_{0.30}MoO_3$ in the incommensurate phase at 143 K.

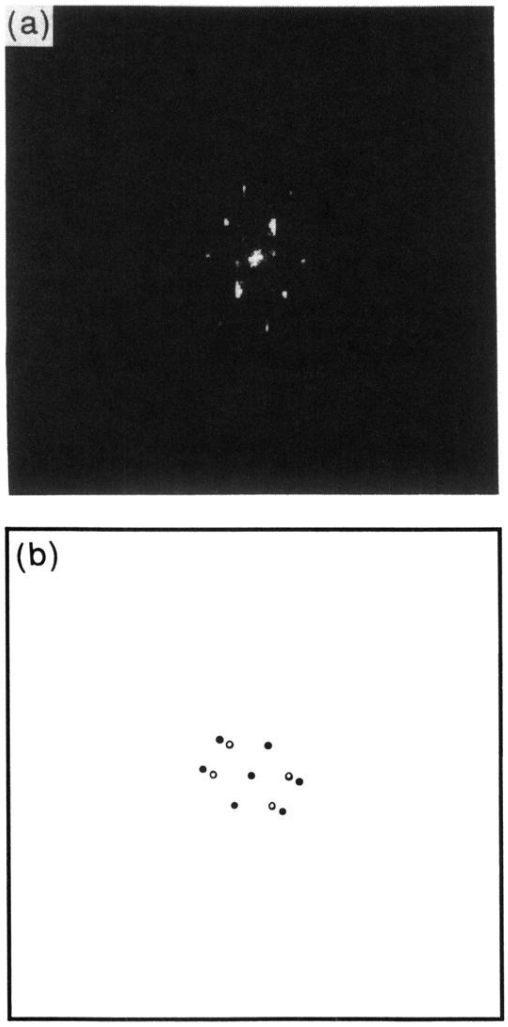

FIG. 6. (a) Fourier transform of Fig. 5 showing the atomic lattice peaks. The two weak peaks nearest the center of the transform are due to 60-Hz noise on the feedback signal. (b) Schematic showing the calculated positions of the atomic lattice peaks (closed circles) and the CDW peaks (open circles).

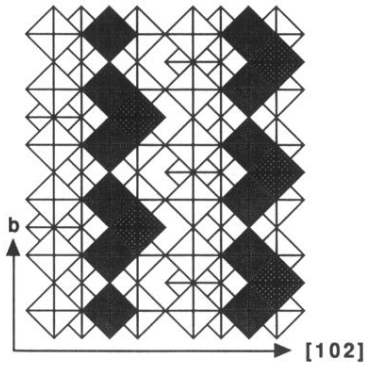

FIG. 9. Structure of the idealized Mo-O octahedra in the topmost unit cell of the cleavage plane. The centers of the "hump" octahedra (the rightmost octahedron in a shaded group of three) are 1.8 Å below the "surface" defined by the b and [102] plane. The gray octahedra have centers 2.4 Å below the "surface."